What, My Ion Gauge is Affecting My Results? LaMnO₃ and Ion Gauge-Activated Propene and Acetone Production from 2-Propanol

Caspar Lant[1, 2, a)] and Aditya Savara[2, b)]

[1)] *Department of Physics, New York University*

[2)] *Chemical Sciences Division, Oak Ridge National Laboratory*

(Dated: 9 August 2019)

Measurements of catalytic activity on well-defined surfaces are often conducted under ultra-high vacuum to enable greater control of their chemical environment. During such measurements, hot cathode ion gauges are typically used to measure the pressure. It has been widely assumed that the impact of these gauges on the studied reactions is negligible. This work shows compelling evidence that the aforementioned assumption is not correct: the presence of a hot cathode ion gauge in an experimental chamber can significantly alter experimental reaction measurement outcomes. The evidence suggests the gauges can even activate dehydrogenation reactions in organic molecules. In mass spectrometry-based measurements of dehydrogenation/dehydration of 2-propanol to acetone/propene, the presence of an ion gauge markedly increased the signals associated with the mass-fragmentation patterns of these products. This particular reaction is of fundamental interest for as-yet inchoate catalysis-based fuel-conversion methods. A hot cathode ion gauge uses a heated filament (typically >1000K) to emit electrons that are recaptured by a collection anode. This type of ion gauge could, in principle excite the electron configuration (through ionization of molecules in the path of its electrons) and/or the thermal modes of molecules that make direct contact with it. We have not yet decoupled these two contributions, making it difficult to determine ascertain exactly which effect is responsible for the apparent increase in production we observe. Consequently, we have devised a plan to thermally excite a collimated stream of moleculesa molecular beamto temperatures in the range of our heated catalyst sample. This will help us to study the mechanism of ion-gauge-activated apparent production of acetone and propene. The proposed heating enhancement to our molecular beam will additionally allow us to study the reaction rates of molecules impinging on a sample as a function of their initial kinetic energies of a broader agenda to characterize the reaction kinetics of catalytic conversions.

I. INTRODUCTION

Perovskite crystals can be effective catalysts for reactions such as the one depicted in FIG. 1 because they lower the activation energy for steps subsequent to when the reactant molecule adsorbs onto sites on the crystal's surface. It is understood that 2-propanol loses its hydroxyl hydrogen as it adsorbs onto the polar-oxide catalyst, as depicted in the lowest portion of FIG 1. The resultant intermediates can either recombine and desorb or form products acetone or propene via dehydrogenation or dehydration, respectively. We are able to kinetically characterize this process by pulsing a gas-phase effusive molecular beam, and following the response of a mass spectrometer. A molecular beam source produces a collimated stream of molecules by filtering them via angle-selection. It uses a microporous glass plate across a pressure differential to do so. In this paper, we present the design of an enhancement to a molecular beam that enables us to control the kinetic energies of the molecules we eject from it. Curiously, we notice that the presence of a powered-on ion gauge in our chamber provokes significant change in the mass spectrometer response to the majority mass fragments of the products we expect from this reaction. The gauge seems to activate some chemical conversion, as well as some amplification effect as a result of ion acceleration from field interactions between the ion gauge and the mass spectrometer's quadropole electron optics.
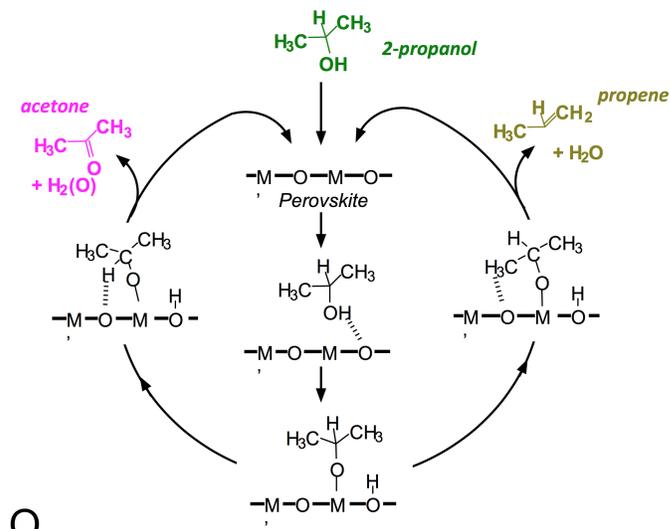

FIG. 1: Reaction Mechanism

[a)]Electronic mail: caspar@nyu.edu

[b)]Electronic mail: savaraa@ornl.gov

II. EXPERIMENTAL

A.   Molecular Beam

We produce an effusive molecular beam in our chamber by first allowing gas-phase molecules of our reagent in question though a glass capillary array, or GCA. The GCA resembles a small wafer of frosted glass, and has is populated with thousands of tens-of-micron-wide tubes passing through it. As molecules from an upper chamber diffuse through the GCA, they are collimated in the direction of its normal. This happens as a result of the molecules being filtered by their $\vec{x}$ and $\vec{y}$ vector components as they collide with the capillary walls in the GCA. This collimation can be tuned by varying the thickness of the GCA and the size of its capillaries, Logic would dictate that a using a thicker GCA would result in better collimation. This beam then makes its way through two differential pumping stages and several plate apertures intended to block the diffuse component of the beam. By the time the molecular beam reaches the sample, its collimated component is relatively high in intensity (by about a factor of 10) as compared to its diffuse (not-beam) component. This is important so as to produce a significant ($\approx 10^{-7}$Torr) effective pressure on the sample from the beam while maintaining UHV in the rest of the chamber.

B.   Ion Gauge Contribution

To convince ourselves that the ion gauge is actually converting 2-propanol to its dehydr(ogen)ated products, we configure our chamber in a "batch reactor" mode. Here we cut off the vast majority of the pumping from the chamber (by closing off the gate valve to a cryopump), and dose it into the 10^{-5}Torr-range with the organic reagent. (In our case 2-propanol.) We subsequently dose the chamber to an equal partial pressure of O_2 to act as a "baseline" in our measurement we assume that oxygen is relatively inert here and will therefore not get consumed by the ion gauge-induced conversion. We use the "total pressure" setting on our mass spectrometer to measure the chamber pressure so as not to pre-expose the reagent (2-propanol) to ion gauge conversion. We allow for the chamber pressure to stabilize by examining the mass spectrometer response, before beginning the pulsing program described in the next section.

III.   RESULTS AND DISCUSSION

From our chamber-as-batch-reactor ion gauge-pulsing experiment described in section II, we see a clear increase in the production of propene- and acetone-associated masses (41 and 43 atomic mass units (or a.m.u.), respectively) as a result of powering on the ion gauge for three minutes between/during 1 minute sampling periods. The fact that we see an increase in the mass spectrometer response of these masses even when the gate valve is opened after the ion gauge pulse has ended sug-

gests that we are seeing genuine conversion, as opposed to some amplification effect onset by an electromagnetic interaction between the ion gauge and the mass spectrometer's quadrupole optics. The results in FIG 2 are obtained by initially dosing the chamber with 2-propanol, allowing its pressure to stabilize, and alternatingly exposing the chamber to 3 minute ion-gauge pulses and not between 1 minute samples of the chamber by manually operating a gate valve. Note: the 2-propanol-associated mass in this figure is deceptively low; we measure this mass "off-peak" so as not to damage the mass spectrometer. The propene-associated mass is 43a.m.u., and the acetone-associated mass is 41a.m.u. The effect of the timing of the ion-gauge-on pulse is explored by varying the "waiting" duration between the end of a pulse and the 1 minute gate valve sampling period. We see in the figure that the longer of a duration between these two events, the smaller the signal of the product masses. Interestingly, the 2-propanol signal (mass 45.5 a.m.u.) does not change intensity across the entire experiment. This, combined with the fact that the signal intensity of the "overlapping" pulse measurement (where the ion gauge is on and the gate valve is open at the same time.) does not change incommensuratelyas compared to the non-overlapping pulse measurement intensities, is evidence that any electromagnetic amplification effect is negligible, and the ion gauge is indeed activating the reactions we describe.

A.   Producing a Heated Molecular Beam

We have recently finished implementing an upgrade that enables us to change the kinetic energy of the reactants incident on the sample by heating them in the molecular beam stage. This will help us to further distinguish the behaviour of our ion gauge from "real" catalytic activity. We control the temperature of the beam by heating the GCA via joule heating of high-resistivity tantalum wire. Particles collimated by the GCA necessarily make thermal contact with it, and–in doing so– equilibrate to a kinetic energy commensurate with the temperature of the GCA:

$$\frac{1}{2}mv_{\mathrm{RMS}}^2 = \frac{2}{3}k_B T_{\mathrm{set}} \qquad (1)$$

We are in the Knudsen Diffusion regime (as opposed to viscous flow), so an application of classical mechanics is permissible. Let's consider a point particle[1] at the upstream mouth of one of the capillaries of our GCA. Let's imagine particle at this location produce an even spherical distribution of trajectories. If you consider the hemisphere of trajectories that have a negative $\bar{z}$-component (into the GCA), the percentage of particles that will pass through the capillary without colliding with its wall is given simply by the aspect ratio of the capillary. This, in the case of a 2mm thick GCA with $20\mu m$-wide capillaries, is around .5%. Naïvely, we consider perfectly inelastic reflections. The percentage of particles that collide only once with the capillary wall is twice this value (you can think about a GCA with half the thickness). Those who
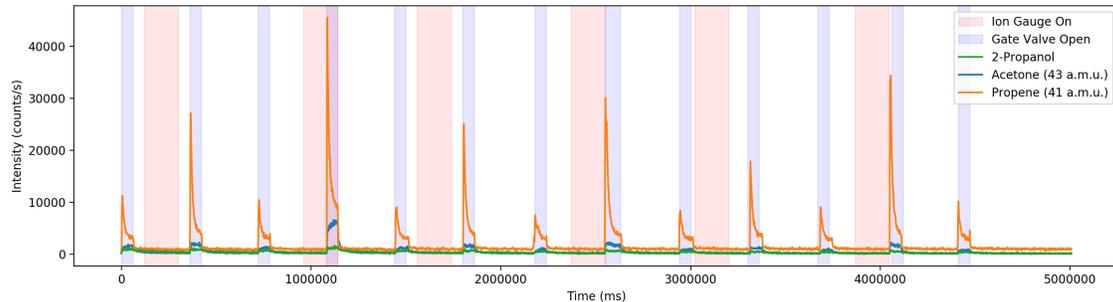
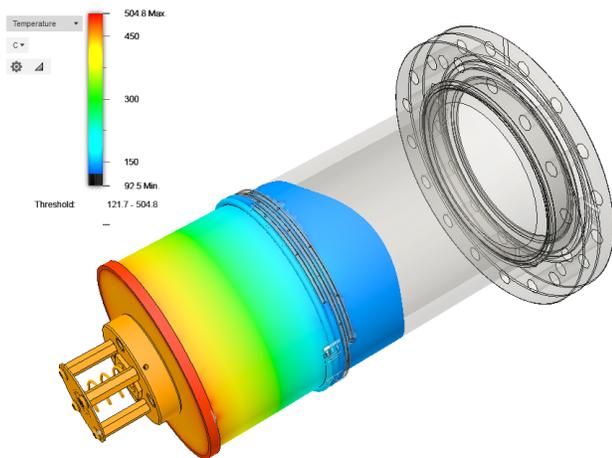FIG. 2: Results of the Ion Gauge Pulsing Experiment

FIG. 3: Temperature Distribution

collide two times are three times the original percentage, and so on. The proportion of thermally equilibrated molecules is given by the following expression, which uses the small-angle approximation ($\tan\theta = \theta$), and n is the number of collisions required for the molecule to reach the v_{RMS} commensurate with the set temperature (true only for small n):

$$1 - (n)\frac{\text{capillary width}}{\text{GCA thickness}} \qquad (2)$$

If we imagine that a particle needs to collide four times[2] with the capillary wall to thermally equilibrate with it[2], the percentage of collimated particles exiting our GCA that are not at the desired kinetic energy (that is, those which are not thermally equilibrated with the GCA) is capped at $\approx 5\%$ as given by Equation 2. The most problematic oversimplification here is the presumption of perfectly specular reflection: that a particle's reflection off a wall can be represented by inverting the sign of the contribution in the direction of the wall's normal to the particle's initial velocity vector. Modeling diffuse reflection would necessitate the use of a cosine distribution[3] at each collision site, which complicates the problem significantly. The good news is that the mean trajectory of particles given by a raised cosine distribution of particles following the scattering event has a vector that points

"upstream" relative to the specular reflection vector. So, equation 2 actually gives us an lower bound on the proportion of molecules with the desired kinetic energy.

1. Power Calculations

Designing the upgrade to achieve a desired temperature of 500 required some additional considerations. A novel feature of the existing molecular beam setup lies the ability to change its colatitude angle. This enables us to precisely align the molecular current out of the GCA through the aperture plates downstream. However, this delicate instrumentation above the molecular beam chamber necessitates that its flange not reach a temperature above 100 °C. Given the length of the "nose" (depicted in FIG. 3)–which contains the high-pressure region of the molecular beam source–and the fact that it operates in a pressure range where convection is negligible, we required a significant heat sink between the 500 °C nose tip and its opposite end. In order to produce a temperature gradient this steep along the stainless steel nose, both the heat source and sink must operate on the order of $\pm$ 600 W. We settled on tantalum resistive heating and active water cooling. From our calculations, 4 coils of water-cooled copper tubing around the 100 mm-diameter nose dissipates 600 W of heat. We consider the interface between the stainless steel nose and the copper tube; and the interface between it and the cooling water flowing through it. The equation below–which assumes isothermal elements and is irrespective of geometry–describes the power dissipated at each interface.

$$P = \frac{A(T_2 - T_1)}{L_1/k_1 + L_2/k_2} \qquad (3)$$

Where A is the contact surface area, T is the temperature of the volume on one side of the interface, L is its length, and k is its heat conduction coefficient[4]. Using Ohm's Law ($V = IR$) and the definition of electrical power ($P = IV$), we calculate the length of tantalum required to meet the ± 600 W constraint forced by the cooling coils. In order to reach a steady state in temperature, the resistive heating must have a power output equal to the power dissipated by the cooling coils. With a calculated linear resistivity of 0.1/m, 34 inches of 30AWG (0.01" diameter)

tantalum wire was required. A different length could have been used with a lower current, but this would mean increasing the voltage, and our safety standards do not permit us to exceed 50V.

IV. CONCLUSIONS

We conclude that ion gauges have the ability to act as 'catalysts' themselves, in converting 2-propanol to acetone and propene products. The beam heating enhancement will enable us to study the reaction rates of molecules impinging on a sample as a function of their initial kinetic energies, as part of a broader agenda to further characterize the reaction kinetics of catalytic conversions.

V. ACKNOWLEDGEMENTS

VI. REFERENCES AND FOOTNOTES

[1] We idealize our molecules as point particles, because their effective size is much smaller than the dimensions of the GCA.

[2] A. Raukema and A. W. Kleyn, Phys. Rev. Lett. **74**, 4333 (1995).

[3] $f(x; \mu, s) = \frac{1}{2s} \left[1 + \cos\left(\frac{x-\mu}{s} \pi \right) \right] = \frac{1}{s} \operatorname{hvc}\left(\frac{x-\mu}{s} \pi \right)$,

where hvc() is the havercosine function, $\frac{1 + \cos\theta}{2}$.

[4] R. Serway and R. J. Bechner, *Physics for Scientists and Engineers* (2000).

[5] V. Nemani, M. umer, and B. Zajec, Vacuum **70**, 523 (2003).

[6] J. H. Singleton, Journal of Vacuum Science & Technology A **19**, 1712 (2001), https://doi.org/10.1116/1.1335679.

[7] P. Redhead, Journal of Vacuum Science & Technology A: Vacuum, Surfaces, and Films **20**, 1667 (2002).

[8] C. Edelmann and I. Kunz, Vacuum **46**, 159 (1995).

[9] C. T. Rettner, D. J. Auerbach, J. C. Tully, and A. W. Kleyn, The Journal of Physical Chemistry **100**, 13021 (1996), https://doi.org/10.1021/jp9536007.

[10] J. Bennett and R. Elsey, Vacuum **44**, 647 (1993), special Issue Selected Proceedings of the 12th International Vacuum Congress (IVC-12) 8th International Conference on Solid Surfaces (ICSS-8).